On the formation and vibronic spectroscopy of α–halobenzyl radicals in a supersonic expansion

Jianlong Yao and Elliot R. Bernstein

On the formation and vibronic spectroscopy of α-halobenzyl radicals in a supersonic expansion

Jianlong Yao and Elliot R. Bernstein
Department of Chemistry, Colorado State University, Fort Collins, Colorado 80523

α-halobenzyl radicals, such as C_6H_5CHCl, C_6H_5CHBr, and $C_6H_5CCl_2$, along with $C_6H_5CH_2$, are generated by pyrolysis and photolysis methods. The mechanism of the formation of the α-halobenzyl radicals in a pyrolysis nozzle is analyzed. Secondary reactions play an important role in the pyrolysis process. Spectra of these supersonic jet cooled radicals are detected by laser induced fluorescence and multiphoton ionization techniques in the $21\,200–23\,500$ cm^{-1} range. Assignment of important vibronic bands of the α-halobenzyl radicals is made by comparing their spectra to that of the benzyl radical and by employing rotational contour and vibrational mode analyses and *ab initio* calculations. The similarity between the vibronic structure of the benzyl radical and α-halobenzyl radicals suggests a similar vibronic coupling scheme for them. Substitution of halogen atoms on the methylene group of the benzyl radical has only a modest affect on the vibronic transitions studied. © *1997 American Institute of Physics.* [S0021-9606(97)01133-1]

I. INTRODUCTION

As the simplest aromatic radical belonging to the family of so called odd alternant hydrocarbons, the benzyl radical has been the subject of numerous spectroscopic and theoretical studies during the last four decades. Most of this attention has been concentrated on the two nearly degenerated excited electronic states $1\,^2A_2$ and $2\,^2B_1$. The unusually weak intensity of these transitions, and their complex vibronic structure due to coupling of the two electronic states, have attracted special attention. Cossart-Magos and co-workers[1(a)–1(c)] definitively assigned the first electronic transition near $22\,000$ cm^{-1} as the $1\,^2A_2 \leftarrow 1\,^2B_1$ transition, and made the first attempt to explain the observed complex vibronic structure through $1\,^2A_2$ and $2\,^2B_1$ vibronic coupling. Recent contributions have mainly come from gas phase studies of jet cooled benzyl radical generated by techniques such as laser photolysis, discharge, pyrolysis and others.[2–6] Miller's group[2] has used laser induced fluorescence (LIF) to detect vibronic and rotational spectra of the benzyl radical. Selco and Carrick[3] have carried out a dispersed emission (DE) analysis of the benzyl radical generated in a corona discharge in a toluene–helium mixture. Our laboratory[4] has used multiphoton ionization (MPI) to study the benzyl radical and related species. Fukushima and Obi[5] have intensively studied dispersed fluorescence from individual vibronic levels of the benzyl radical. Eiden and Weisshaar[6] have devoted their effort to both MPI and pulsed field ionization (PFI) study of benzyl radicals. In a recent paper,[6(d)] these latter authors have compiled most of the available experimental and theoretical data, and modeled a nice scheme for the vibronic coupling mechanism in the $1\,^2A_2$ and $2\,^2B_1$ states of the benzyl radical.

Substituted benzyl radicals have also been subjected to many studies in order to elucidate a number of important radical properties; these include electron withdrawing, electron donating, resonance, and isotope substituent effects, as well as others. Earlier condensed phase studies have been discussed in a review article by Johnston.[7] Recent gas phase research has included a number of systems: p-fluorobenzyl, p-cyanobenzyl, p-xylyl, and α-duterated benzyl radicals by Obi and co-workers[5] using LIF and DE; Selco and Carrick[3(c)] have studied o-, m, and p-xylyl by the same approach they used for the benzyl radical; and Miller and co-workers[2(b),2(c)] have studied o-, m, and p-xylyl system to elucidate both their vibronic and rotational spectra using LIF. The latter authors also have observed gas phase spectra of diphenyl, α-chlorodiphenyl, triphenyl methyl radicals and others.[2(d)] Using MPI, our lab[4] has studied duterated benzyl, and nitrogen substituted radicals (such as picolyl and lutidyl radicals). Weisshaar and co-workers[6(c),6(d)] also studied deuterated benzyl radicals in detail by LIF, MPI, and PFI techniques.

In this paper, we report on α-chlorobenzyl (C_6H_5CHCl), α-dichlorobenzyl ($C_6H_5CCl_2$), α-bromo benzyl (C_6H_5CHBr) along with the benzyl radical generated by 193 nm ArF laser photolysis and pyrolysis in a supersonic jet expansion. The well studied benzyl radical serves as a reference for both the experimental conditions and spectroscopic analysis. Excitation spectra in $430–465$ nm wavelength range are recorded for these radicals by using LIF and MPI. The formation of α-halobenzyl radicals has been analyzed. The vibronic structures of α-halobenzyls have been analyzed through comparison to that of the benzyl radical.

The notation of symmetry species and vibrational modes adopted by different people have varied with time. We choose to use Mulliken's notation for all symmetry specifications in order to be consistent with the standard coordinate system adopted in theoretical calculations.

The axis system used in this work is indicated in Fig. 1. $C_6H_5CH_2$ and $C_6H_5CCl_2$ have a C_{2v} symmetry, while C_6H_5CHCl and C_6H_5CHBr have a C_s symmetry. Symmetry species A_2, B_1, and B_2 in C_{2v} reduce to A'', A'', and A', respectively, in C_s. Since the electronic states of different radicals under study all originate from the seven delocalized π electrons common to all of them, we expect that certain similarities exist for these systems. For easy comparison, we
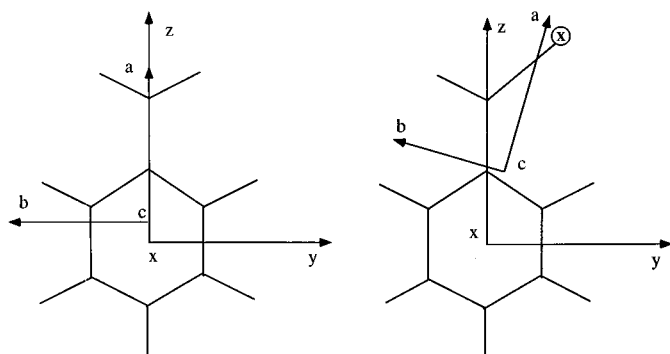
FIG. 1. Schematic axis systems adopted in this work. The figures on the left and right represent axis systems for $C_6H_5CH_2(C_6H_5CCl_2)$ and C_6H_5CHX (X=Cl or Br), respectively. The origins of the (x,y,z) axis system in different radicals are always located at the center of the rings. (a,b,c) axis systems are main rotational axis systems with origins at centers of mass. The x and c axes are pointing out of paper.

choose the same x, y, z axis orientations for both C_{2v} and C_s symmetries. The main rotational axes a, b, and c for C_6H_5CHCl and C_6H_5CHBr are oriented differently as indicated. As for the vibrational modes, we still use traditional notation[9] so that a comparison for similar vibrational modes among various benzyl radical related species is feasible.

II. PROCEDURES

A. Experiment

Precursors used in the work include $C_6H_5CH_2X$ (X=H, Cl, Br, I), $C_6H_5CHCl_2$, and $C_6H_5CCl_3$. They are all purchased from Aldrich.

Either photolysis, pyrolysis, or both methods are tried to decompose these compounds to generate the appropriate reactive intermediates. Spectroscopic detection techniques used for photolysis and pyrolysis are MPI and LIF, respectively.

The experimental setup and detail procedure of photolysis-MPI has been demonstrated in a previous paper.[4(b)] Briefly, a 193 nm ArF excimer laser with an energy of roughly 80 mJ/pulse is lightly focused onto the exit region of an R. M. Jordan pulsed valve operating at 10 Hz. Helium

is used as the expansion gas at a backing pressure of 80–100 psi. The radicals formed are collisionally cooled and travel downstream to a pair of ion extraction plates, where they are excited to certain vibronic states by a DCR IIA Nd:Yag pumped dye laser (spectra physics) and then ionized by a second similar laser. The ions created are extracted by a 250 V potential difference and accelerated into a time-of-flight mass spectrometer at 4 keV total kinetic energy. Mass resolved detection of the ionized radicals is achieved by using a Galieo Electro-Optics multichannel-plate (MCP) detector at the end of a 1.5 m flight tube. Various coumarin dyes are used for the excitation laser, while F548 (frequency doubled) is used for the ionization laser. These two laser pulses are spatially and temporally overlapped.

Figure 2 shows a schematic diagram of the pyrolysis nozzle. This device is built based on a design of Chen et al.[10] and Ellison et al.[11] The central part of the nozzle is a 2 mm o.d., 1 mm i.d. Hexoloy SA (Carborundum Corp., Niagara Falls, NY) SiC tube of length 2.5 cm. The SiC tube is heated in an evacuated quartz capsule at 1100 °C for 2 h prior to mounting on the nozzle to reduce its resistance from several hundred kΩ to below 10 kΩ.

A 3 mm o.d., 2 mm i.d. Al_2O_3 tube with a length of 1.2–1.4 cm is used for both electrical and thermal insulation between the nozzle stainless steel front plate and the SiC tube. One or two 2 in.×2 in.×0.02 in. Al_2O_3 disks are loosely slip fit on the Al_2O_3 tube to act as a heat shield for the rest of the nozzle. Al_2O_3 cement is used to fix and seal the tube connections. On the SiC tube, two graphite disks (machined from 3/8 in. diam Poco ZXF-5Q rod) are slip fit tightly on the SiC tube to serve as electrodes. Tantalum clamps are used as connections between the graphite electrodes and Mo wires. The SiC tube is in series with three 200 W parallel connected incandescent light bulbs. SiC has a negative temperature coefficient. When the temperature increases, the resistance of the SiC tube decreases to $\sim$ 10 Ω. The light bulbs thus serve as a current limiter in the heater circuit. Typically, when 60 V ac is applied to the circuit, 50 W (2 A×25 V) power is supplied to the SiC tube, and the temperature in the heating zone between the two graphite electrodes is measured at around 1000 °C by a tungsten
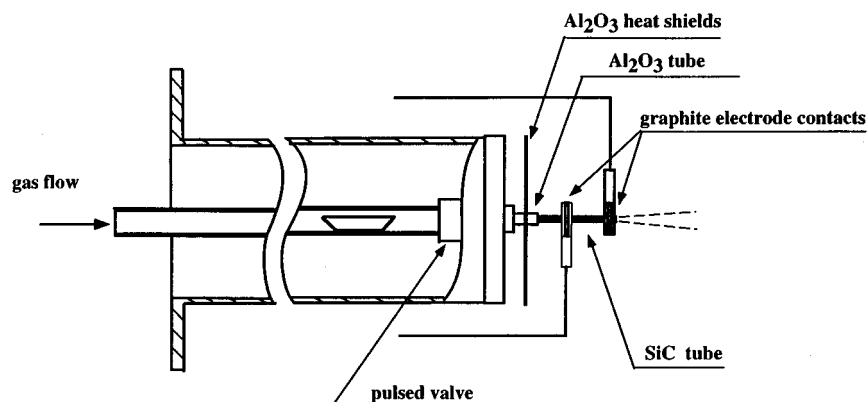

FIG. 2. A schematic diagram of a pyrolysis nozzle.

thermocouple attached to the tube. When precursor molecules pass through the heating zone at high enough temperature, they thermally decompose.

The resistance of the SiC tube keeps dropping slowly in usage. To keep roughly the same temperature, one has to increase the voltage applied gradually so that the power supplied to the tube is roughly constant. This is accomplished by hand regulation of a variac voltage controller in the circuit.

Radicals exiting the nozzle tip are excited by the DCR II dye laser 1–to 1.5 cm downstream. The fluorescence light is collected by a 15 cm focal length lens (f/3) and then monitored by a Hamamatsu R943-02 or RCA 31034A photomultiplier tube connected to an EG&G ORTEC 9301 preamplifier.

B. Theory

All the radicals under study have 36 normal modes. Ground state frequency calculations are performed for C_6H_5CHCl, $C_6H_5CCl_2$ as well as $C_6H_5CCl_2$ on the level of ROHF/6-31G** using the GAUSSIAN 94 program.[12] Correlation of modes of different radicals is made by carefully comparing mode structures depicted according to calculated displacement of atoms.

Ground state rotational constants are calculated by optimizing the ground state geometry of the radicals. A ROMP2/6-311G** level calculation is performed for benzyl, while a ROMP2/6-31G** level calculation is done for C_6H_5CHCl, $C_6H_5CCl_2$.

The introduction of heavy halo atoms into the benzyl radicals makes high level calculation a formidable task. We did not calculation the excited state structures of the α-halobenzyls.

For $C_6H_5CH_2$ and C_6H_5CHCl, CIS/6-31G and CIS/6-311G** calculations are performed to obtain some information on their electronic transitions. Although these low level calculations do not give accurate transition energies and predict a reversed order for the two closely lying excited states, 1^2A_2 and 2^2B_1 in the benzyl radical, they still reveal some valuable information; this includes the electronic configurations for excited states, orientation of electric dipole moments, and a relative comparison of the oscillator strength for different transitions.

For rotational band contour analysis, we choose to follow previous examples[13] employing trial and error simulation. Checking through the available rotational constants for various substituted benzyl radicals,[1–3,5] we notice that the changes are typically 2%–5% for $(A''-A')/A''$, and 0–3% for $(B''-B')/B''$ and $(C''-C')/C''$, respectively, in which A'', B', C'' and A', B', C' are ground and excited states rotational constants, respectively. We start with the calculated ground state rotational constants, guess a temperature value (10–20 K for pyrolysis generated radicals) and a resolution value (0.5–1.0 for our low resolution spectra), then vary A', B', and C' values within the above range. The band contour simulation program used is written by Martinez[13] for asymmetric rigid rotors.
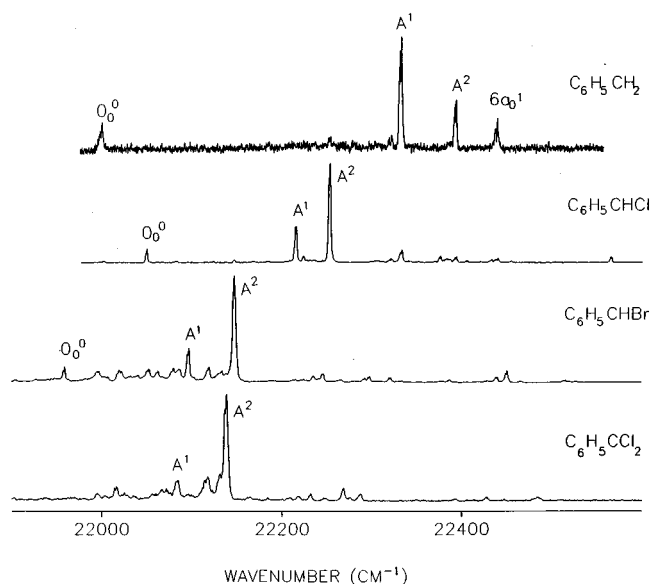

FIG. 3. Pyrolysis-LIF spectra of the benzyl and α-halobenzyl radicals.

III. RESULTS

A. Generation of radicals

$C_6H_5CH_3$, $C_6H_5CH_2I$, $C_6H_5CH_2Br$, and $C_6H_5CH_2Cl$ are used to generate $C_6H_5CH_2$ for the photolysis. The first three precursors give only $C_6H_5CH_2$, while the latter one gives mostly $C_6H_5CH_2$ along with some C_6H_5CHCl. The photolysis of $C_6H_5CHCl_2$ gives mostly C_6H_5CHCl with some amount of $C_6H_5CCl_2$, while that of $C_6H_5CCl_3$ gives only $C_6H_5CCl_2$. All these products are as expected and are readily identified in their own specific mass channels.

While pyrolysis of $C_6H_5CH_3$, $C_6H_5CH_2I$, $C_6H_5CCl_3$ give the same results as photolysis does, pyrolysis of the other precursors ($C_6H_5CH_2Cl$, $C_6H_5CH_2Br$, and $C_6H_5CHCl_2$) shows somewhat different behavior. At first, pyrolysis of $C_6H_5CH_2Cl$ gives both $C_6H_5CH_2$ and C_6H_5CHCl with comparable intensity in the LIF spectrum. Actually this has been observed in an earlier pyrolysis/LIF experiment,[14] but peaks belonging to C_6H_5CHCl were assigned as $C_6H_5CH_2$ hot bands. After about half an hour of continuous pyrolysis, C_6H_5CHCl becomes the only product detectable by LIF generated from the $C_6H_5CH_2Cl$ precursor. The same behavior is found for the $C_6H_5CH_2Br$ precursor; eventually C_6H_5CHBr becomes the only detected radical by LIF from this precursor. The pyrolysis of $C_6H_5CHCl_2$ produces both C_6H_5CHCl and $C_6H_5CCl_2$ with comparable intensity of each spectrum.

B. Spectra

1. Overview

LIF spectra have been taken for $C_6H_5CH_2$, C_6H_5CHCl, $C_6H_5CCl_2$, and C_6H_5CHBr generated by pyrolysis, while MPI spectra have been taken for the first three species following photolysis. Spectra are shown in Figs. 3 and 4.

Pyrolysis/LIF spectra are taken in the 21 900 $-22\,600\ cm^{-1}$ range. These spectra are of rotationally hotter molecules than those derived from the photolysis/MPI pro-
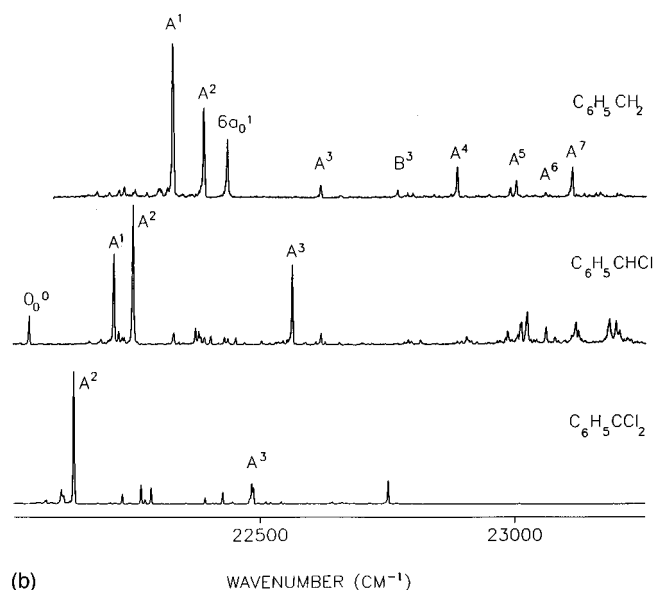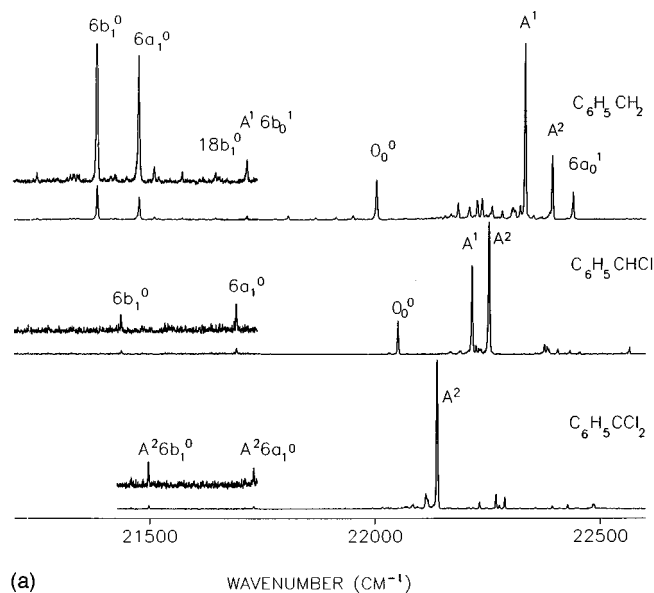
FIG. 4. (a) Photolysis-MPI spectra of the benzyl and α-halobenzyl radicals in the C460 dye tuning range. (b) Photolysis-MPI spectra of the benzyl and α-halobenzyl radicals in the C440 dye tuning range.

FIG. 5. Experimental and simulated rotational band contours of the benzyl and α-halobenzyl radicals. (a) and (b) $6a_0^1$, and A^2 bands of $C_6H_5CH_2$. (c) A^2 band of $C_6H_5CCl_2$; (d), (e), and (f) 0_0^0, A^1, and A^2 bands of C_6H_5CHCl. See Table I for structural parameters used in simulations. Resolution used is 0.8 cm^{-1}. Temperatures are 10 K for the benzyl radical and 15 K for α-halobenzyl benzyl radicals, respectively.

tional frequency calculations for the ground state radicals and CIS calculations for the electronic transitions of $C_6H_5CH_2$ and C_6H_5CHCl.

2. Rotational band contours

Band contours of some prominent vibronic features from the spectra of various radicals are shown in Fig. 5 along with simulated contours. With a resolution of 0.8 cm^{-1} and a rotational temperature of 10 K, the $1^2A_2 \leftarrow 1^2B_1 0_0^0$, $1^2A_2 6a_0^1$, A^1, and A^2 band contours of $C_6H_5CH_2$ are well fit using the rotational constants from either Miller's,[2(b)] or our own calculation, as listed in Table I. The first two bands are of B type and the latter two are of A type, since they are originated from $a(z)$ and $b(y)$ polarized vibronic transitions, respectively. Band contours of A^2 and $1^2A_2 6a_0^1$ are shown in Figs. 5(a) and 5(b) along with simulations. For our low resolution spectra, it appears that rotational band type is the most important factor in determining the shape of a band. Small variations of rotational constants do not show up obviously in the simulated band contours. This should also be true for the other radicals studied.

The rotational band contour of the $C_6H_5CCl_2$ feature at $22\,131.3$ cm^{-1} is simulated as an A type band [Fig. 5(c)] using parameters listed in Table I along with 0.8 cm^{-1} resolution and a 15 K rotational temperature. On the other hand, the rotational band contour of C_6H_5CHCl cannot be simulated as a pure A or B type band. Instead, mixed band types are fit to all four prominent features in its spectrum. These fitting parameters are listed in Table I. Again the fit resolution is 0.8 cm^{-1} and the rotational temperature is 15 K. Some of the simulations are shown in Figs. 5(d)–5(f). The mixed band type behavior clearly indicates that the electronic tran-

cess. This is due to the intrinsic characteristics of the pyrolysis method and the absence of a skimmer in the beam path. The rotational temperature for these spectra is estimated at around 15 K. The relatively hotter spectra show clearer rotational band contours that are helpful in assigning the vibronic structure of the radicals.

Photolysis/MPI spectra are taken in both the C460 and C440 dye tuning ranges, as shown in Figs. 4(a) and 4(b), respectively. Note that the A^3 peak of C_6H_5CHCl in Fig. 4(a) appears much weaker than that in Fig. 4(b) due to the decline of the C460 dye laser intensity. Assignment of $C_6H_5CH_2$ features are made based on Refs. 1, 3–6. We attempt to assign the spectra of the α-halobenzyl radicals based on (1) the similarity of the spectra of all four radicals, especially the pyrolysis/LIF spectra, (2) rotational band type, and (3) vibra-
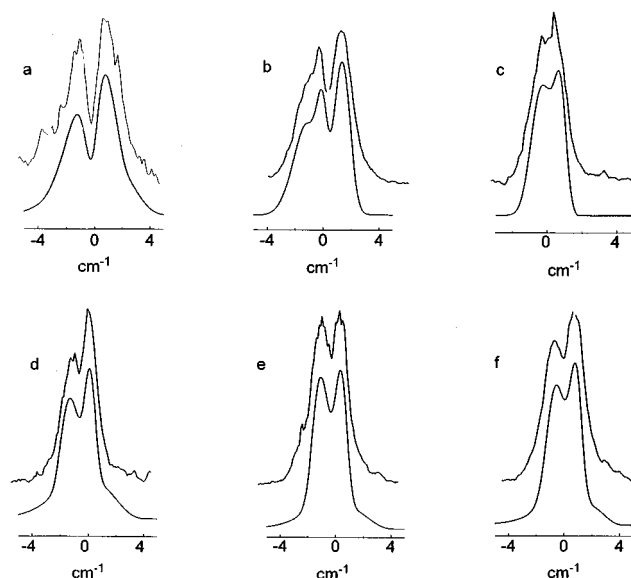
TABLE I. Parameters used in band contour simulation.[a]

Radical	A''	B''	C''	Band	ΔA	ΔB	ΔC	Band type
	cm^{-1}				$\times 10^{-4}$ cm^{-1}			
$C_6H_5CH_2$	0.184 55	0.089 68	0.060 35	$1^2A_2 6a_0^1$	39.5	17.0	12.0	B
	(0.184 16	0.090 13	0.058 72)[b]		(37.3	17.0	11.0)[b]	
				A^1	54.0	17.0	13.0	A
					(53.3	16.7	13.0)[b]	
C_6H_5CHCl	0.165 86	0.032 07	0.026 88	$2^2A''O_0^0$	58.6	10.7	8.7	$0.5A + 0.5B$
				A^1	68.6	0.0	0.0	$0.7A + 0.3B$
				A^2	78.6	6.7	4.7	$0.7A + 0.3B$
$C_6H_5CCl_2$	0.071 65	0.027 03	0.019 63	A^2	40.2	10.3	6.2	A

[a]A'', B'', and C'' are calculated ground state rotational constants. ΔA is defined as $A''-A'$, etc.
[b]Data in parentheses are from Ref. 2(b).

sition dipole moment of C_6H_5CHCl is not oriented in the same direction as either the a or b rotational axis. This result is supported by the *ab initio* CIS calculation discussed below. This is a reasonable finding considering that the electronic transition of C_6H_5CHCl under study has essentially originated from the seven π electrons of the skeleton carbon atoms, and should therefore largely retain the C_{2v} character of $C_6H_5CH_2$. On the other hand, the orientation of main rotational axes a, b, and c is changed upon substitution of Cl for H due to the significant change in molecular mass distribution.

3. Benzyl radical

All of the observed features of the benzyl radicals and some of their vibronic band type assignments are listed in Table II. As shown in Figs. 4(a) and 4(b) and listed in Table II, more than 10 hot bands to the red of the origin and more than 40 bands to the blue of origin have been observed by photolysis/MPI detection. The vibronic bands observed to the blue of the $1^2A_2 \leftarrow 1^2B_1$ origin are essentially the same as observed previously by various groups.[4–6] Important vibronic bands are those relatively high intensity features assigned as A^1, A^2, $1^2A_2 6a_0^1$, and A^3. The A^1, A^2, and A^3 bands gain their intensity mainly from 2^2B_1 state through vibronic coupling.[1,5(c),6(d)]

Assignment of the hot bands follows those made by Selco and Carrick,[3(a)] and Obi *et al.*[5(d)] Notice that $1^2A_2 6a_1^0$ and $1^2A_2 6b_1^0$ hot bands have intensities comparable to $1^2A_2 \leftarrow 1^2B_1$ origin transition.

4. α-chlorobenzyl radical

All the bands observed for the α-chlorobenzyl radical are listed in Table III, as well as some assignments. The spectra of C_6H_5CHCl and $C_6H_5CH_2$ are apparently somewhat similar.

Table IV shows some CIS calculation results for the ground to excited state transitions of C_6H_5CHCl and $C_6H_5CH_2$. As expected, the calculations predict excitation energies more than 100% higher than experimental values, and also predict a reversed order for the 2^2B_1 and 1^2A_2 excited states in $C_6H_5CH_2$. Nevertheless, the calculated tran-

sition properties, such as the transition electric dipole moments and oscillator strength, still give a reasonable qualitative picture for the lower energy electronic transitions of these radicals. In the case of $C_6H_5CH_2$, the calculated transition electric dipole moments of the 1^2A_2, $2^2B_1 \leftarrow 1^2B_1$ transitions are along $b(Y)$ and $a(Z)$ axes, respectively, as is observed experimentally. The oscillator strength of the $2^2B_1 \leftarrow 1^2B_1$ transition is 7.7 and 12.6 times that of the $1^2A_2 \leftarrow 1^2B_1$ transition, as calculated by 6-31G and 6-311G** basis sets. This is consistent with the relative electronic transition strength factor of $S_{B-X}^2/S_{A-X}^2 = 15$ estimated by Eden and Weisshaar.[6(d)]

As for C_6H_5CHCl, the CIS calculation indicates a first excited state with A' symmetry [B_2 in C_{2v} for $\sigma(yz)$ preserved as in Fig. 1] and a weak electronic transition to this state from the ground state which is polarized along the $c(X)$ axis direction. The existence of this state is not evident in the spectroscopic range accessed in these studies in any of the benzyl-type radicals. The ground state and the second and third excited states all have A'' symmetry in the C_s group. The calculated transition electric dipole moments in Table IV actually show that the $2A'' \leftarrow 1A''$ and $3A'' \leftarrow 1A''$ transitions are polarized along Y and Z axes (see Fig. 1), respectively. Further, the ratio of oscillator strength for the $3A'' \leftarrow 1A''$ transition over the $2A'' \leftarrow 1A''$ transition is 5.5. These results suggest that the $2A'' \leftarrow 1A''$ and $3A'' \leftarrow 1A''$ transitions are the analogs of the $1^2A_2 \leftarrow 1^2B_1$ and $2^2B_1 \leftarrow 1^2B_1$ transition in $C_6H_5CH_2$, respectively. The similarity between the observed vibronic structures of $C_6H_5CH_2$ and C_6H_5CHCl, supported by this theoretical analysis, lead us to assign the transition at 22 045.5 cm^{-1} as the origin transition of $2^2A'' \leftarrow 1^2A''$ of the α-chlorobenzyl radical, and the three strong vibronic bands at 22 209.2, 22 247.0, and 22 557.6 cm^{-1} as the A^1, A^2, and A^3 bands, in analogy to those of the benzyl radical. These latter three bands have a mixed envelope character of 70% A and 30% B type character.

The band character of 70% A and 30% B of the A^1, A^2, and A^3 bands in C_6H_5CHCl means that the corresponding vibronic transition dipole moments are distributed 70% along the a axis and 30% along the b axis. This distribution

TABLE II. Vibronic bands observed for the benzyl radical 2^2B_1, $1^2A_2 \leftarrow 1^2B_1$ transitions.

Wave number (cm^{-1})	Spacing from 0_0^0 (cm^{-1})	Assignment[a] (band type)
21 247.5	−750.8	$A^2 6a_1^0 6b_1^0$
21 381.2	−617.1	$6b_1^0(A)$
21 473.4	−524.9	$6a_1^0(B)$
21 507.3	−491.0	$A^1 1_1^0$
21 568.4	−429.9	$A^2 1_1^0$
21 641.7	−356.6	$18b_1^0$
21 710.3	−288.0	$A^1 6b_1^0$
21 772.8	−225.5	$A^2 6b_1^0$
21 802.3	−196.0	$A^1 6a_1^0$
21 863.1	−135.2	$A^2 6a_1^0$
21 908.8	−89.5	$6a_1^0$
21 946.0	−52.3	
21 998.3	0.0	$0_0^0(B)$
22 178.7	180.4	
22 203.8	205.5	
22 221.0	222.7	
22 231.5	233.2	
22 253.7	255.4	
22 276.3	278.0	
22 300.0	301.7	
22 316.3	318.0	
22 326.1	327.8	$A^1(A)$
22 386.7	388.4	$A^2(A)$
22 431.9	433.6	$6a_0^1(B)$
22 502.6	504.3	
22 530.0	531.7	
22 569.2	570.9	
22 614.2	615.9	$A^3(A)$
22 653.6	655.3	
22 671.4	673.1	
22 688.6	690.3	
22 701.8	703.5	
22 721.6	723.3	
22 738.4	740.1	
22 764.4	766.1	$B^3(B)$
22 783.5	785.2	
22 792.9	794.6	
22 816.0	817.7	
22 836.6	838.3	
22 868.4	870.1	
22 881.0	882.7	$A^4(A)$
22 918.0	919.7	
22 942.6	944.3	
22 963.2	964.9	
22 984.0	985.7	
22 996.7	998.4	$A^5(A)$
23 017.4	1019.1	
23 027.0	1028.7	
23 034.2	1035.9	
23 054.3	1056.0	$A^6(A)$
23 105.8	1107.5	$A^7(A)$
23 114.6	1116.3	
23 119.1	1120.8	
23 139.4	1141.1	

TABLE II. (*Continued.*)

Wave number (cm^{-1})	Spacing from 0_0^0 (cm^{-1})	Assignment[a] (band type)
23 152.9	1154.6	
23 161.9	1163.6	
23 173.0	1174.7	
23 186.7	1188.4	
23 195.0	1196.7	
23 201.3	1203.0	
23 286.3	1288.0	$A^8(A)$
23 292.7	1294.4	$A^9(A)$
23 302.1	1303.8	
23 317.7	1319.4	

[a]Notation for vibronic bands to the red of the origin is adopted from Ref. 1, while that for vibronic bands A^1 through A^9 to the blue of the origin is adopted from Refs. 4–6.

TABLE III. Vibronic bands of C_6H_5CHCl.

Wave number (cm^{-1})	Spacing from 0_0^0 (cm^{-1})	Assignment (band type)
21 432.5	−612.0	$6b_1^0$
21 686.8	−358.4	$6a_1^0$
22 044.5	0.0	0_0^0 (50% A+50% B)
22 160.8	116.3	
22 182.0	137.5	
22 208.5	164.0	A^1 (70% A+30% B)
22 218.0	173.5	
22 227.0	182.5	
22 246.6	202.1	A^2 (70% A+30% B)
22 325.4	280.9	
22 368.7	324.2	
22 375.3	330.8	
22 385.7	341.2	
22 398.3	353.8	
22 424.7	380.2	
22 431.8	387.3	
22 447.2	402.7	
22 464.2	419.7	
22 497.2	452.7	
22 557.5	513.0	A^3 (70% A+30% B)
22 582.6	538.1	
22 602.8	568.4	
22 621.2	576.7	
22 649.1	604.6	
22 784.6	740.1	
22 808.0	763.5	
22 888.8	844.3	
22 898.9	854.4	
22 979.5	935.0	
23 005.2	960.7	
23 017.2	972.7	
23 054.4	1010.2	
23 071.6	1027.1	
23 112.1	1067.6	
23 118.0	1073.5	
23 171.9	1127.4	
23 191.4	1146.9	

is almost exactly the distribution calculated for the transition dipole moment of the $3A'' \leftarrow 1A''$ transition. This correspondence supports the parallel between the $C_6H_5CH_2$ and the C_6H_5CHCl spectra.

Table V shows the correlation between some of the im-

TABLE IV. Ground to excited states electronic transition dipole moments and oscillator strengths of $C_6H_5CH_2$ and C_6H_5CHCl, determined by CIS/6-31G and CIS/6-311G** calculations.

Radical	Basis set	Excited state	Electronic dipole moments[a] (a.u.)			Oscillator strength (a.u.)	Transition energy (eV)	
			a	b	c		Calc	Expt
$C_6H_5CH_2$	6-31G	$2\,^2B_1$	0.226 70	0	0	0.007 7	6.1	
		$1\,^2A_2$	0	0.079	0	0.001 1	6.3	
	6-311G**	$2\,^2B_1$	$-0.296\ 3$	0	0	0.012 6	5.9	2.727 4
		$1\,^2A_2$	0	0.084 5	0	0.001 0	5.9	
C_6H_5CHCl	6-31G	$1\,^2A'$	0	0	$-0.116\ 7$	0.002 0	5.9	
		$2\,^2A''$	0.098 4	$-0.204\ 9$	0	0.007 8	6.2	2.733 2
		$3\,^2A''$	$-0.489\ 0$	$-0.196\ 4$	0	0.043 0	6.3	

[a]Values presented are projections of electric dipole moments along a, b, and c axes (see Fig. 1).

portant vibrational modes of C_6H_5CHCl and $C_6H_5CH_2$. A careful comparison of the calculated mode structure of the two radicals indicates that out-of-plane modes (with a'' symmetry in C_6H_5CHCl, and a_2 or b_1 symmetry in $C_6H_5CH_2$) and those modes with little or no motion in α-H(Cl) atom positions remain essentially the same for the two radicals, while some of the in-plane modes, which involve large amplitude motion in α-H(Cl) atom positions, change dramatically for the two radicals.

The $6a$ (a_1 symmetry) mode is one of those that changes significantly between the two radicals. Two a' modes (calculated as 339.0 and 557.1 cm^{-1}) of C_6H_5CHCl show some characteristics of the $6a$ mode of $C_6H_5CH_2$. The lower frequency mode of these two is also observed as a hot band at 21 686.8 cm^{-1}, with a frequency of 358.4 cm^{-1}.

The $6b$ (b_1 symmetry) mode has little motion at the two atoms bound to the α-carbon, and should therefore be preserved in C_6H_5CHCl. Indeed, we have observed this mode as a hot band at 21 432.5 cm^{-1}. The ground state frequency of this mode for C_6H_5CHCl is 612.7 cm^{-1} compared to 617.1 cm^{-1} for $C_6H_5CH_2$.

5. α-bromobenzyl radical

C_6H_5CHBr is generated by the pyrolysis process from the only available precursor $C_6H_5CH_2Br$. The spectra is presented in Fig. 3. All bands observed for this radical are listed in Table VI. The vibronic structure is apparently similar to that of C_6H_5CHCl. We assign the 21 952.6 cm^{-1} feature as the origin band of the transition analogous to the $2\,^2A'' \leftarrow 1\,^2A''$ transition of C_6H_5CHCl. The two features at 22 090.0 cm^{-1} and 22 140.5 cm^{-1} are apparently the analogs of the A_1, A_2 bands of C_6H_5CHCl. This assignment is also supported by the similarity between rotational band contours of the corresponding vibronic features of C_6H_5CHCl and C_6H_5CHBr.

6. α-dichlorobenzyl radical

The vibronic bands observed for $C_6H_5CCl_2$ are listed in Table VII. Only one feature in the photolysis/MPI spectrum of the α-dichlorobenzyl radical is intense, as shown in Fig. 4. This makes a straightforward assignment of the $C_6H_5CCl_2$ spectrum rather problematic.

TABLE V. Symmetry and ground state energies (cm^{-1}) of some vibrational modes of the benzyl and α-substituted benzyl radicals.[a]

Mode		$C_6H_5CH_2$		C_6H_5CHCl		$C_6H_5CCl_2$	
Wilson[b]	Weisshaar[c]	Symm.	Calc (expt)	Symm.	Calc (expt)	Symm.	Calc (expt)
11	36	b_1	211.5	a''	208.0	b_1	168.5
18b	29	b_2	338.6(356.6)	a'	169.5	b_2	153.9
16a	17	a_2	413.1	a''	408.3	a_2	408.2
6a	13	a_1	514.3(524.9)	a'[d]	339.0(358.4)	a_1	385.9(406.3)
				a'[d]	557.1		
6b	28	b_2	612.0(617.1)	a'	608.3(612.0)	b_2	622.1(639.3)
12a	12	a_1	1014.3(987)[e]	a'	1011.8	a_1	1037.0
8b	21	b_2	1594.7(1549)[e]	a'	1595.3	b_2	1604.2

[a]All the frequencies determined by ROHF/6-31G**//6-31G** calculations are scaled to 90% of those actually calculated.
[b]References 3(a) and 9.
[c]References 6(c) and 6(d).
[d]Both modes show some $6a$ characteristic.
[e]Experimental values from Ref. 3(a).

TABLE VI. Vibronic bands of C_6H_5CHBr.

Wave number (cm^{-1})	Spacing from 0_0^0 (cm^{-1})	Assignment
21 952.6	0.0	0_0^0
21 990.7	38.1	
22 013.9	61.3	
22 045.7	93.1	
22 055.7	103.1	
22 072.5	119.9	
22 080.3	127.7	
22 089.9	137.3	A^1
22 112.1	159.5	
22 126.0	173.4	
22 140.5	187.9	A^2
22 209.2	256.6	
22 217.7	265.1	
22 228.8	276.2	
22 239.3	286.7	
22 246.2	293.6	
22 259.5	306.9	
22 285.2	332.6	
22 290.8	338.2	
22 313.9	361.3	
22 380.0	427.4	
22 412.4	459.8	
22 421.2	468.6	
22 432.1	479.5	
22 443.0	490.4	
22 459.0	506.4	
22 507.5	554.9	
22 512.7	560.1	

TABLE VII. Vibronic bands of $C_6H_5CCl_2$.

Wave number (cm^{-1})	Assignment (band type)
21 492.0	$A^2 6b_1^0$
21 588.0	
21 706.3	
21 725.0	$A^2 6a_0^1$
21 793.0	
21 927.3	
21 988.0	
21 010.8	
22 022.9	
22 063.9	
22 079.0	A^1
22 088.0	
22 106.4	
22 131.3	$A^2(A)$
22 224.9	
22 239.3	
22 216.2	
22 269.1	
22 281.1	
22 349.0	
22 386.5	
22 421.2	
22 440.5	
22 477.5	A^3
22 480.8	
22 505.1	
22 514.3	
22 534.3	
22 634.1	
22 652.8	
22 662.4	
22 745.0	

The similarity between the pyrolysis/LIF spectra (Fig. 3) of $C_6H_5CCl_2$ and C_6H_5CHBr suggests that $C_6H_5CCl_2$ may have a vibronic structure similar to that of C_6H_5CHBr; i.e., a low oscillator strength transition origin may exist for $C_6H_5CCl_2$ in the vicinity of the transition origin of C_6H_5CHBr at 21 952.6 cm^{-1}, with features at 22 079.0 cm^{-1} and 22 131.3 cm^{-1} assigned as vibronic bands. The band at 22 131.3 cm^{-1} is an A type band and a comparison to the benzyl radical vibronic structure suggests that the missing origin is a $1^2A_2 \leftarrow 1^2B_1$ origin. The features at 22 079.0 cm^{-1} and 22 131.3 cm^{-1} are possibly the A^1 and A^2 vibronic structures as assigned for the other radicals.

The feature at 22 477.5 cm^{-1} in the $C_6H_5CCl_2$ spectrum is most likely related to the A^3 feature of $C_6H_5CH_2$ and C_6H_5CHCl [see Fig. 4(b)]. Weak hot bands at 21 492 and 21 725 cm^{-1} are 639 cm^{-1} and 406.3 cm^{-1} to the red of the A^2 peak; they can be assigned as $A^2 6b_1^0$ and $A^2 ba_1^0$, respectively, based on a ground state frequency calculation and a similar mode correlation analysis applied to C_6H_5CHCl (see Table V).

7. Isotopes

Photolysis/MPI spectra have been recorded for all the Cl isotopmers of C_6H_5CHCl and $C_6H_5CCl_2$. The signal intensity ratios are 3:1 for $C_6H_5CH^{35}Cl$:$C_6H_5CH^{37}Cl$, and 9:6:1 for $C_6H_5C^{35}Cl_2$:$C_6H_5C^{35}Cl^{37}Cl$:$C_6H_5C^{37}Cl_2$, as expected. Unlike the significant change in vibronic structure caused by deuteration of the benzyl radical,[4(b),5(c),6(c),6(d)] the vibronic structure and band contours of these α-chlorobenzyl isotopmers are essentially identical. The isotope shift of peak positions are on the order of 0.1 cm^{-1}, compared to that of 0.14 cm^{-1} found for the first singlet–singlet electronic transition origin of ^{35}Cl- and ^{37}Cl–C_6H_5.[15]
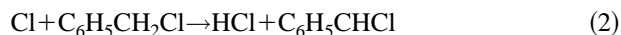
IV. DISCUSSION

A. Radical generation by pyrolysis
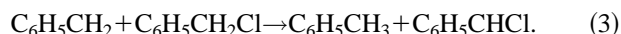
The results of the pyrolysis of $C_6H_5CH_2Cl$, $C_6H_5CH_2Br$, and $C_6H_5CHCl_2$ are somewhat unexpected, since the C–X (X=Cl,Br) bond is the weakest one in these precursors. One would anticipate that the C–X bond would break first and give mainly the $C_6H_5CH_2$ radical, rather than C_6H_5CHCl (Br) from $C_6H_5CH_2Cl$ (Br), and (C_6H_5CHCl + $C_6H_5CCl_2$) from $C_6H_5CHCl_2$. The observed results are understandable, however, if one considers the process in the pyrolysis tube in detail. As already studied in earlier work,[10,11] we know that the pressure drop for the gas flow in the SiC tube is small, and the dwell time in a one inch long tube is on the order of a few tens of μs. Taking $C_6H_5CH_2Cl$ as an example, at a temperature as high as 1000 K, one can expect the following reaction occurs first:

$$C_6H_5CH_2Cl \rightarrow C_6H_5CH_2 + Cl. \tag{1}$$
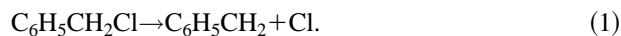
As an estimate, we take the residence time of precursor molecules in the hot zone as 20 μs, the mean pressure in the tube as 1 atm, and the precursor molecules as comprising 1% of total gas flow. Then on average each $C_6H_5CH_2$ and Cl formed may experience more than 10 collisions with $C_6H_5CH_2Cl$. Secondary reactions can therefore occur in the following manner:
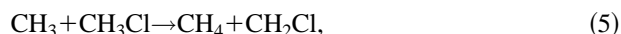
$$Cl + C_6H_5CH_2Cl \rightarrow HCl + C_6H_5CHCl \qquad (2)$$

and

$$C_6H_5CH_2 + C_6H_5CH_2Cl \rightarrow C_6H_5CH_3 + C_6H_5CHCl. \qquad (3)$$

According to Bensen,[16] reaction (2) has a ΔH of -22 kcal/mol and the activation energy of ~ 1 kcal/mol. As for reaction (3), we know that the bond energy of $C_6H_5CH_2$–H is about 86 kcal/mol and that of C_6H_5CHCl–H should be lower. So this reaction is also an exothermic radical metathesis reaction, and its activation energy should also be small.[16] Therefore, both reactions (2) and (3) are possible in the pyrolysis process.

Actually, in earlier studies[17] on the pyrolysis of CH_3Cl, similar radical mechanisms were proposed for the initial stages of decomposition,

$$CH_3Cl \rightarrow CH_3 + Cl, \qquad (4)$$

$$CH_3 + CH_3Cl \rightarrow CH_4 + CH_2Cl, \qquad (5)$$

and

$$Cl + CH_3Cl \rightarrow HCl + CH_2Cl. \qquad (6)$$

As for $C_6H_5CH_2Br$ and $C_6H_5CHCl_2$, although energetically reactions similar to reactions (2) and (3) are not quite so favorable, one can still expect similar reactions take place.

In a series of studies[18] on the pyrolysis of $C_6H_5CH_2Cl$, $C_6H_5CH_2Br$, and $C_6F_5CH_2Br$ in a $C_6H_5CH_3$ flow, the species C_6H_5CHCl, C_6H_5CHBr, or C_6F_5CHBr are not identified. This is probably due to the large amount of $C_6H_5CH_3$ compare to the studied molecules (100 times as much). As already known, $C_6H_5CH_3$ is very effective in removing various radicals by the mechanism

$$C_6H_5CH_3 + R \rightarrow C_6H_5CH_2 + HR, \qquad (7)$$

in which R represents radical. Therefore, X, C_6H_5CHX (X=Cl, Br), or C_6F_5CHBr formed (if any) should be removed by $C_6H_5CH_3$, leaving only $C_6H_5CH_2$ as a major radical species, while in our case, $C_6H_5CH_2Cl(Br)$ and $C_6H_5CHCl_2$ serve as the major radical scavengers in Eq. (7) above.

B. Vibronic structure and substituent effects

The benzyl radical and many of its α-substituted analogs are alternant hydrocarbons with 7 π electrons. The first electronic transition ($1^2A_2 \leftarrow 1^2B_1$) of the benzyl radical is symmetry allowed, but has only weak transition intensity. This is due to a so called ''accidental forbiddenness,'' an accidental cancellation of two dominant terms in the expression for the transition dipole moment.[19,5(d)] The complicated and relatively stronger vibronic features to the blue of the origin

transition are mainly caused by vibronic coupling. It is believed[5(d),6(d)] that the $1^2A_2 6a_0^1$ band gains its intensity mainly from Herzberg–Teller coupling of the first excited state 1^2A_2 to higher $^2A_2$ states through the $6a$ mode of a_1 symmetry, while the features marked as A^1, A^2, and A^3 bands (Figs. 3 and 4) gain their intensity through the mixing of certain b_2 symmetry modes ($6b$, $11+16a$, and $8b$ for A^1 and A^2, and $6b$ and $8b$ for A^3) of the 1^2A_2 state with the closely lying $2^2B_1 0^0$ state (zero vibrational level). A similar cancellation of moments happens for 2^2B_1 state, as well; nevertheless, the oscillator strength of the $2^2B_1 \leftarrow 1^2B_1$ transition is considerably larger (ca. a factor of 10) than that of the $1^2A_2 \leftarrow 1^2B_1$ transition.

The direct impact of substituents on the vibronic structure of substituted benzyl radicals can be seen in the following observations: (1) change in energy of electronic states, specifically, changes in the transition energy of the first electronic transition, and the separation between the 1^2A_2 and 1^2B_1 states or even a reversal of order of the two states; (2) change in transition intensity to these states, i.e., the extent of the accidental cancellation of transition moments; and (3) changes in vibrational modes.

Condensed phase[7] and recent supersonic jet[5(e)] studies indicated that strong substituent effects in the p-cyanobenzyl radical make the 2^2B_1 state the first excited state. Active modes characterizing the first electronic transition in the p-cyanobenzyl radical ($2^2B_1 \leftarrow 1^2B_1$) are totally symmetric ones with the frequencies higher than 800 cm^{-1}; active modes characterizing the first electronic transition in the benzyl radical ($1^2A_2 \leftarrow 1^2B_1$) are, on the other hand, nontotally symmetric modes $6b$, $8b$ and totally symmetric mode $6a$ (all with the frequency lower than 800 cm^{-1}). Even stronger effects are observed for the α-cyanobenzyl radical spectrum. The p-fluorobenzyl[5(b),1(d)] radical presents another example of a strong substituent effect. In this case, the 2^2B_1 electronic state is significantly higher in energy than the 1^2A_2 electronic state. Therefore vibronic coupling between the two states becomes negligible and the vibronic structure remains nearly the same as that of p-fluorotoluene. Furthermore, the accidental forbiddenness of the $1^2A_2 \leftarrow 1^2B_1$ transition no longer exists. O-, m-, and p-xylyl radicals[1(d),2(c),3(c)] also show rather strong substituent effects. The origin transitions for these latter radicals are shifted about 300 cm^{-1}, but the vibronic structures of these transitions are heavily perturbed, especially by the internal torsion motion of methyl group.

Consider, now the spectra of the α-halo substituted benzyl radicals. As is analyzed earlier, the observed electronic transitions of these radicals are either the same as, or closely analogous to, that of the parent benzyl radical, and their transition origins are all weak and lie within 100 cm^{-1} of those of the benzyl radical and each other. This means that the substitution of a halogen on the α-carbon has only a very small effect on the relative energy levels of the electronic states studied, and does not change the accidentally forbidden nature of the first electronic transition observed.

Considering the similarity between the vibronic structures of the benzyl radical and α-halobenzyl radicals, i.e., the

weak electronic origin transition in the vicinity of 22 000 cm^{-1} and the rather strong vibronic transitions to the blue of origin, we tend to believe the vibronic bands of the α-halobenzyl radical originate from a vibronic coupling scheme similar to that found for the benzyl radical.

As just mentioned, $11+16a$, $6b$ and $8b$ modes are believed to be the main modes that couple the $1\,^2A_2$ and $2\,^2B_1$ states to form the A^1, A^2, and A^3 vibronic bands of the benzyl radical, while $18b$ has only a minor contribution to this $C_6H_5CH_2$ coupling scheme but significant contribution to some vibronic bands found for $C_6D_6CD_2$. The mode analysis discussed above points out that little or no α-carbon H or X motion is present for the 11, $16a$, $6b$ modes. From Table V we can see that the ground state energy of these modes are all essentially unchanged in C_6H_5CHCl and $C_6H_5CCl_2$, while the α-group bending mode $18b$ is significantly reduced in energy upon H/X substitution. The same trend should hold for excited states. Now if we compare the shifts of the A^1, A^2, and A^3 features with respect to the origins of the radicals studied, we can see an obvious decrease in the shifts upon substitution (see Tables II, III, VI, VII). Apparently, this can not be caused by $11+16a$, $6b$ or $8b$ modes which remain almost unchanged. The possible source of this decrease could be either from a reduction of the separation between the first two excited states, or from an increase of the contribution from the $18b$ mode with a much reduced energy, or both. A detail dispersed emission or PFI study of the strong vibronic features similar to that done for the benzyl radical will help in elucidating these probabilities.

The two vibrational modes $6a$ and $6b$ merit more attention because they are both very active in benzyl radical spectrum. The parentage of these two modes can be traced back to the doubly degenerated mode 6 of benzene. In the benzyl radical, $6b$ is one of the major modes involved in the vibronic coupling process between the $1\,^2A_2$ and $2\,^2B_1$ states. $1\,^2A_2 6a_0^1$, and hot bands $6a_1^0$ and $6b_1^0$ all have intensity comparable to or even larger than the origin band. In ring substituted benzyl radicals, both $6a$ and $6b$ modes are subjected to significant change caused by the motion of the substituent atoms or groups. A reverse order of frequency is suggested by Cossart-Magos *et al.*[1(d)] and Selco *et al.*[3(c)] in the case of xylyl radicals. In the p-xylyl radical, $6b$ and $6a$ are believed to have frequencies of 458.3 cm^{-1} and 637.3 cm^{-1}, respectively, compared to 617.1 cm^{-1} and 524.9 cm^{-1}, respectively, observed for the benzyl radical.

As is mentioned earlier, while analyzing the spectra of C_6H_5CHCl and $C_6H_5CCl_2$ in Sec. III B, the motion of α-substituted halo-atoms in the $6a$ mode cause drastic change in both mode pattern and energy. In the case of C_6H_5CHCl, $6a$ has actually lost its clear identity, and two modes both show the characteristics of $6a$. In the $6b$ mode the halo-atoms move almost not at all, and thus the mode experiences little change upon substitution, as is shown both in the experimental and calculated results (Table V). Both $6a$ and $6b$ are not as active in α-halobenzyl radicals as they are in benzyl. This can be seen by the fact that no prominent vibronic band can be assigned as $6a_0^1$, and their hot bands

have much smaller intensity in α-halobenzyl radicals compared to that found for the benzyl radical.

While it is obvious that the change in both mode pattern and energy of the $6a$ and $6b$ modes in substituted benzyl radicals depends on the change in the amplitude of the motion of each atom and group (especially the substituent), the cause of the change in their vibronic band intensity is not as clear.

V. CONCLUSION

In this work, both photolysis and pyrolysis techniques have been used to generate the α-halobenzyl radicals C_6H_5CHCl, C_6H_5CHBr, and $C_6H_5CCl_2$. Secondary reactions dominate the later stages in the pyrolysis generation of C_6H_5CHCl and C_6H_5CHBr.

The gas phase spectra of these radicals are obtained unambiguously by both LIF and MPI detection techniques. Assignment of important vibronic bands is made by comparison of the spectra of these radicals to that of the benzyl radical, and with the help of rotational contour analysis, vibrational mode analysis, and *ab initio* calculations.

Substitution of halogen on the methylene group of the benzyl radical has only a modest effect on the vibronic transitions studied. The vibronic structure of the three radicals are similar to one another and are not very different from that of the benzyl radical. This observation suggests a similar vibronic coupling scheme for these α-halobenzyl radicals. The reduced separation between the $1\,^2A_2 \leftarrow 1\,^2B_1$ transition origin and strong vibronic bands A^1 and A^2 may be caused by the change in detailed vibronic coupling mechanisms. The first two electronic states are closer to one another and the $18b$ mode is more active for these α-substituted benzyl radicals than for the benzyl radical.

Changes in vibrational modes depend on whether or not the substituted α-halo atoms are involved in any large amplitude motion. Vibronically active modes $6b$, $8b$, 11, $16a$ remain essentially unchanged upon substitution, while the totally symmetric mode $6a$ is one of the most changed low energy modes.

ACKNOWLEDGMENTS

[1](a) C. Cossart-Magos and S. Leach, J. Chem. Phys. **56**, 1534 (1972); (b) **64**, 4006 (1976); (c) C. Cossart-Magos and W. Goetz, J. Mol. Spectrosc. **115**, 366 (1986); (d) C. Cossart-Magos and D. Cossart, Mol. Phys. **65**, 627 (1988).

[2](a) S. C. Foster and T. A. Miller, J. Phys. Chem. **93**, 5986 (1989), and

references therein; (b) T. D. Lin, X. Tan, T. M. Cerny, J. M. Williamson, D. W. Cullin, and T. A. Miller, Chem. Phys. **203**, 167 (1992); (c) T. D. Lin and T. A. Miller, J. Phys. Chem. **94**, 3554 (1990); (d) T. D. Lin, C. P. Damo, J. R. Dunlop, and T. A. Miller, Chem. Phys. Lett. **168**, 349 (1990).

[3] (a) J. I. Selco and P. G. Carrick, J. Mol. Spectrosc. **137**, 13 (1989); (b) **139**, 449 (1990); (c) **173**, 277 (1995).

[4] (a) H. S. Im and E. R. Bernstein, J. Chem. Phys. **95**, 6326 (1991); (b) R. Disselkamp and E. R. Bernstein, *ibid*. **98**, 4339 (1993); (c) J. Phys. Chem. **98**, 7260 (1994); (d) J. A. Bray and E. R. Bernstein (unpublished).

[5] (a) H. Hiratsuka, K. Mori, H. Shizuka, M. Fukushima, and K. Obi, Chem. Phys. Lett. **157**, 35 (1989); (b) M. Fukushima and K. Obi, J. Chem. Phys. **93**, 8488 (1990); (c) **96**, 4224 (1992); (d) Chem. Phys. Lett. **242**, 443 (1995); (e) M. Fukushima, K. Saito, and K. Obi, J. Mol. Spectrosc. **180**, 389 (1996).

[6] (a) G. Eiden and J. C. Weisshaar, J. Phys. Chem. **95**, 6194 (1991); (b) G. Eiden, F. Weinhold, and J. C. Weisshaar, J. Chem. Phys. **95**, 8665 (1991); (c) G. Eiden, K-T. Lu, J. Badenhoop, F. Weinhold, and J. C. Weisshaar, *ibid*. **104**, 8886 (1996); (d) G. Eiden and J. C. Weisshaar, *ibid*. **104**, 8896 (1996).

[7] L. J. Johnston, Chem. Rev. **93**, 251 (1993).

[8] R. S. Mulliken, J. Chem. Phys. **23**, 1997 (1955).

[9] (a) E. B. Wilson, Jr., J. C. Decius, and P. C. Cross, *Molecular Vibrations* (Dover, New York, 1995); (b) E. B. Wilson, Phys. Rev. **45**, 706 (1934).

[10] D. W. Khon, H. Clauberg, and P. Chen, Rev. Sci. Instrum. **63**, 4003 (1992).

[11] H. W. Rohrs, C. T. Wickham-Jones, G. B. Ellison, D. Berry, and B. M. Angrow, Rev. Sci. Instrum. **66**, 2430 (1995).

[12] GAUSSIAN 94, M. J. Frisch, G. W. Trucks, H. B. Schlegel, P. M. W. Gill, B. G. Johnson, M. A. Robb, J. R. Cheeseman, T. A. Keith, G. A. Petersson, J. A. Montgomery, K. Raghavachari, M. A. Al-Laham, V. G. Zakrzewski, J. V. Ortiz, J. B. Foresman, J. Cioslowski, B. B. Stefanov, A. Nanay-akkara, M. Challancombe, C. Y. Peng, P. Y. Ayala, W. Chen, M. W. Wong, J. L. Andres, E. S. Replogle, R. Gomperts, R. L. Martin, D. J. Fox, J. S. Binkley, D. J. Defrees, J. Baker, J. P. Stewart, M. Head-Gordon, C. Gonzalez, and J. A. Pople, Gaussian Inc., Pittsburgh, Pennsylvania, 1995.

[13] R. Pereira, I. Alava, F. Castano, and M. T. Martinez, J. Chem. Soc. Faraday Trans. **90**, 2443 (1994).

[14] J. R. Dunlop, J. Karolczak, and D. J. Clouthier, Chem. Phys. Lett. **151**, 362 (1988).

[15] A. De la Cruz, J. Campos, and M. Ortiz, J. Mol. Spectrosc. **180**, 305 (1996).

[16] S. W. Bensen, *Thermochemical Kinetics*, 2nd ed. (Wiley, New York, 1976), p. 236.

[17] (a) A. E. Shilov and R. D. Sabirova, Zh. Fiz. Khim. **33**, 1365 (1959); (b) K. A. Holbrook, Trans. Faraday Soc. **57**, 2151 (1961); (c) R. J. Robinson and K. A. Holbrook, *Unimolecular Reactions* (Wiley–Interscience, New York, 1971), p. 258.

[18] (a) M. Szwarc, B. N. Ghosh, and A. H. Sehon, J. Chem. Phys. **18**, 1142 (1950); (b) R. J. Kominar, M. J. Krech, and S. J. W. Price, Can. J. Chem. **58**, 1906 (1980).

[19] (a) M. J. S. Dewar and H. C. Longuet-Higgins, Proc. Phys. Soc. (London) A **67**, 759 (1954); (b) H. C. Longuet-Higgins and J. A. Pople, **68**, 591 (1955).